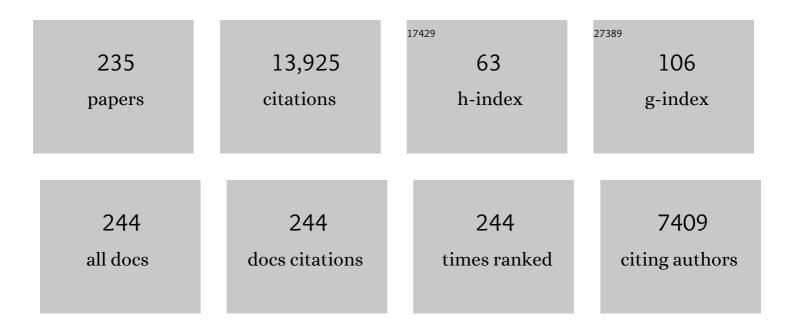
Stan S Solomon

List of Publications by Year in descending order

Source: https://exaly.com/author-pdf/4928976/publications.pdf Version: 2024-02-01



#	Article	IF	CITATIONS
1	Contributions of Stratospheric Water Vapor to Decadal Changes in the Rate of Global Warming. Science, 2010, 327, 1219-1223.	6.0	975
2	Ancient Geodynamics and Global-Scale Hydrology on Mars. Science, 2001, 291, 2587-2591.	6.0	453
3	Solar EUV Experiment (SEE): Mission overview and first results. Journal of Geophysical Research, 2005, 110, .	3.3	448
4	Comparison of COSMIC ionospheric measurements with groundâ€based observations and model predictions: Preliminary results. Journal of Geophysical Research, 2007, 112, .	3.3	266
5	New Perspectives on Ancient Mars. Science, 2005, 307, 1214-1220.	6.0	265
6	The Whole Atmosphere Community Climate Model Version 6 (WACCM6). Journal of Geophysical Research D: Atmospheres, 2019, 124, 12380-12403.	1.2	261
7	The effect of particle precipitation events on the neutral and ion chemistry of the middle atmosphere: II. Odd hydrogen. Planetary and Space Science, 1981, 29, 885-893.	0.9	257
8	The auroral 6300 Ã emission: Observations and modeling. Journal of Geophysical Research, 1988, 93, 9867-9882.	3.3	257
9	Modeling the whole atmosphere response to solar cycle changes in radiative and geomagnetic forcing. Journal of Geophysical Research, 2007, 112, .	3.3	230
10	Solar extreme-ultraviolet irradiance for general circulation models. Journal of Geophysical Research, 2005, 110, .	3.3	228
11	The role of molecular hydrogen and methane oxidation in the water vapour budget of the stratosphere. Quarterly Journal of the Royal Meteorological Society, 1988, 114, 281-295.	1.0	224
12	Development and Validation of the Whole Atmosphere Community Climate Model With Thermosphere and Ionosphere Extension (WACCMâ€X 2.0). Journal of Advances in Modeling Earth Systems, 2018, 10, 381-402.	1.3	213
13	The October 28, 2003 extreme EUV solar flare and resultant extreme ionospheric effects: Comparison to other Halloween events and the Bastille Day event. Geophysical Research Letters, 2005, 32, .	1.5	212
14	The Structure of Mercury's Magnetic Field from MESSENGER's First Flyby. Science, 2008, 321, 82-85.	6.0	194
15	The effect of particle precipitation events on the neutral and ion chemistry of the middle atmosphere—I. Odd nitrogen. Planetary and Space Science, 1981, 29, 767-774.	0.9	185
16	Seasonal variation of thermospheric density and composition. Journal of Geophysical Research, 2009, 114, .	3.3	183
17	Anomalously low solar extremeâ€ultraviolet irradiance and thermospheric density during solar minimum. Geophysical Research Letters, 2010, 37, .	1.5	171
18	Reflectance and Color Variations on Mercury: Regolith Processes and Compositional Heterogeneity. Science, 2008, 321, 66-69.	6.0	167

#	Article	IF	CITATIONS
19	Total volcanic stratospheric aerosol optical depths and implications for global climate change. Geophysical Research Letters, 2014, 41, 7763-7769.	1.5	159
20	Initial results from the coupled magnetosphere ionosphere thermosphere model: magnetospheric and ionospheric responses. Journal of Atmospheric and Solar-Terrestrial Physics, 2004, 66, 1411-1423.	0.6	144
21	Thermosphere extension of the Whole Atmosphere Community Climate Model. Journal of Geophysical Research, 2010, 115, .	3.3	144
22	TIMED Doppler Interferometer: Overview and recent results. Journal of Geophysical Research, 2006, 111, .	3.3	140
23	Geology of the Caloris Basin, Mercury: A View from MESSENGER. Science, 2008, 321, 73-76.	6.0	140
24	Global observations of nitric oxide in the thermosphere. Journal of Geophysical Research, 2003, 108, .	3.3	134
25	Thermal escape of carbon from the early Martian atmosphere. Geophysical Research Letters, 2009, 36, .	1.5	127
26	MESSENGER Observations of the Composition of Mercury's Ionized Exosphere and Plasma Environment. Science, 2008, 321, 90-92.	6.0	121
27	Initial results from the coupled magnetosphere–ionosphere–thermosphere model: thermosphere–ionosphere responses. Journal of Atmospheric and Solar-Terrestrial Physics, 2004, 66, 1425-1441.	0.6	120
28	Observations and simulations of the ionospheric and thermospheric response to the December 2006 geomagnetic storm: Initial phase. Journal of Geophysical Research, 2008, 113, .	3.3	120
29	The 630 nm dayglow. Journal of Geophysical Research, 1989, 94, 6817-6824.	3.3	116
30	Causes of low thermospheric density during the 2007-2009 solar minimum. Journal of Geophysical Research, 2011, 116, n/a-n/a.	3.3	116
31	The Global-Scale Observations of the Limb and Disk (GOLD) Mission. Space Science Reviews, 2017, 212, 383-408.	3.7	105
32	Thermospheric Density: An Overview of Temporal and Spatial Variations. Space Science Reviews, 2012, 168, 147-173.	3.7	102
33	lonospheric annual asymmetry observed by the COSMIC radio occultation measurements and simulated by the TIEGCM. Journal of Geophysical Research, 2008, 113, .	3.3	99
34	Trends in the Neutral and Ionized Upper Atmosphere. Space Science Reviews, 2012, 168, 113-145.	3.7	98
35	A model of nitric oxide in the lower thermosphere. Journal of Geophysical Research, 2002, 107, SIA 22-1-SIA 22-12.	3.3	95
36	An Estimate of the Sun'sROSATâ€PSPC Xâ€Ray Luminosities UsingSNOE‣XP Measurements. Astrophysic Journal, 2003, 593, 534-548.	al 1.6	95

#	Article	IF	CITATIONS
37	Empirical model of nitric oxide in the lower thermosphere. Journal of Geophysical Research, 2004, 109,	3.3	93
38	Parameterization of monoenergetic electron impact ionization. Geophysical Research Letters, 2010, 37, .	1.5	93
39	The anomalous ionosphere between solar cycles 23 and 24. Journal of Geophysical Research: Space Physics, 2013, 118, 6524-6535.	0.8	93
40	Behavior of the <i>F</i> ₂ peak ionosphere over the South Pacific at dusk during quiet summer conditions from COSMIC data. Journal of Geophysical Research, 2008, 113, .	3.3	92
41	Annual/semiannual variation of the ionosphere. Geophysical Research Letters, 2013, 40, 1928-1933.	1.5	90
42	Global 3â€D ionospheric electron density reanalysis based on multisource data assimilation. Journal of Geophysical Research, 2012, 117, .	3.3	85
43	Electron impact ionization: A new parameterization for 100 eV to 1 MeV electrons. Journal of Geophysical Research, 2008, 113, .	3.3	84
44	Initial Observations by the GOLD Mission. Journal of Geophysical Research: Space Physics, 2020, 125, e2020JA027823.	0.8	80
45	Ionospheric electric field variations during a geomagnetic storm simulated by a coupled magnetosphere ionosphere thermosphere (CMIT) model. Geophysical Research Letters, 2008, 35, .	1.5	78
46	Calculated and observed climate change in the thermosphere, and a prediction for solar cycle 24. Geophysical Research Letters, 2006, 33, .	1.5	77
47	Mercury's Exosphere: Observations During MESSENGER's First Mercury Flyby. Science, 2008, 321, 92-94.	6.0	77
48	Solar Extreme Ultraviolet Irradiance Measurements During Solar Cycle 22. Solar Physics, 1998, 177, 133-146.	1.0	76
49	Progress in observations and simulations of global change in the upper atmosphere. Journal of Geophysical Research, 2011, 116, n/a-n/a.	3.3	76
50	Globalâ€Scale Observations of the Equatorial Ionization Anomaly. Geophysical Research Letters, 2019, 46, 9318-9326.	1.5	76
51	Measurements of the solar soft X-ray irradiance by the Student Nitric Oxide Explorer: First analysis and underflight calibrations. Journal of Geophysical Research, 2000, 105, 27179-27193.	3.3	75
52	Ionospheric response to the initial phase of geomagnetic storms: Common features. Journal of Geophysical Research, 2010, 115, .	3.3	75
53	Effect of solar soft X-rays on the lower ionosphere. Geophysical Research Letters, 2001, 28, 2149-2152.	1.5	74
54	Global distribution and interannual variations of mesospheric and lower thermospheric neutral wind diurnal tide: 1. Migrating tide. Journal of Geophysical Research, 2008, 113, .	3.3	74

#	Article	IF	CITATIONS
55	Artificial plasma cave in the low″atitude ionosphere results from the radio occultation inversion of the FORMOSATâ€3/COSMIC. Journal of Geophysical Research, 2010, 115, .	3.3	71
56	Relative importance of horizontal and vertical transports to the formation of ionospheric stormâ€enhanced density and polar tongue of ionization. Journal of Geophysical Research: Space Physics, 2016, 121, 8121-8133.	0.8	71
57	Global modeling of thermospheric airglow in the far ultraviolet. Journal of Geophysical Research: Space Physics, 2017, 122, 7834-7848.	0.8	71
58	Flare location on the solar disk: Modeling the thermosphere and ionosphere response. Journal of Geophysical Research, 2010, 115, .	3.3	70
59	Auroral production of nitric oxide measured by the SNOE satellite. Geophysical Research Letters, 1999, 26, 1259-1262.	1.5	69
60	Variability of thermosphere and ionosphere responses to solar flares. Journal of Geophysical Research, 2011, 116, n/a-n/a.	3.3	68
61	Coupled model simulation of a Sun-to-Earth space weather event. Journal of Atmospheric and Solar-Terrestrial Physics, 2004, 66, 1243-1256.	0.6	67
62	The ionospheric and thermospheric response to CMEs: Challenges and successes. Journal of Atmospheric and Solar-Terrestrial Physics, 2007, 69, 77-85.	0.6	67
63	Solar Flare and Geomagnetic Storm Effects on the Thermosphere and Ionosphere During 6–11 September 2017. Journal of Geophysical Research: Space Physics, 2019, 124, 2298-2311.	0.8	67
64	Auroral particle transport using Monte Carlo and hybrid methods. Journal of Geophysical Research, 2001, 106, 107-116.	3.3	64
65	Geomagnetic influence on aircraft radiation exposure during a solar energetic particle event in October 2003. Space Weather, 2010, 8, n/a-n/a.	1.3	64
66	Midlatitude nighttime enhancement in <i>F</i> region electron density from global COSMIC measurements under solar minimum winter condition. Journal of Geophysical Research, 2008, 113, .	3.3	63
67	XUV Photometer System (XPS): Improved Solar Irradiance Algorithm Using CHIANTI Spectral Models. Solar Physics, 2008, 250, 235-267.	1.0	62
68	The quenching rate of O(1D) by O(3P). Planetary and Space Science, 1986, 34, 1143-1145.	0.9	61
69	Whole Atmosphere Simulation of Anthropogenic Climate Change. Geophysical Research Letters, 2018, 45, 1567-1576.	1.5	60
70	TIMED Doppler interferometer (TIDI) observations of migrating diurnal and semidiurnal tides. Journal of Atmospheric and Solar-Terrestrial Physics, 2006, 68, 408-417.	0.6	59
71	Global distribution, seasonal, and inter-annual variations of mesospheric semidiurnal tide observed by TIMED TIDI. Journal of Atmospheric and Solar-Terrestrial Physics, 2011, 73, 2482-2502.	0.6	59
72	The Twoâ€Dimensional Evolution of Thermospheric â~O/N ₂ Response to Weak Geomagnetic Activity During Solarâ€Minimum Observed by GOLD. Geophysical Research Letters, 2020, 47, e2020GL088838.	1.5	59

#	Article	IF	CITATIONS
73	Model simulations of global change in the ionosphere. Geophysical Research Letters, 2008, 35, .	1.5	58
74	Tomographic inversion of satellite photometry. Applied Optics, 1984, 23, 3409.	2.1	57
75	<title>TIMED solar EUV experiment</title> . , 1998, 3442, 180.		56
76	The effects of Corotating interaction region/High speed stream storms on the thermosphere and ionosphere during the last solar minimum. Journal of Atmospheric and Solar-Terrestrial Physics, 2012, 83, 79-87.	0.6	56
77	A new Fabry-Perot interferometer for upper atmosphere research. , 2004, 5660, 218.		54
78	Solar-terrestrial coupling: Solar soft X-rays and thermospheric nitric oxide. Geophysical Research Letters, 1999, 26, 1251-1254.	1.5	53
79	Global distribution and interannual variations of mesospheric and lower thermospheric neutral wind diurnal tide: 2. Nonmigrating tide. Journal of Geophysical Research, 2008, 113, .	3.3	53
80	Solar flare impacts on ionospheric electrodyamics. Geophysical Research Letters, 2012, 39, .	1.5	53
81	The dissociative recombination of O ₂ ⁺ : The quantum yield of O(¹S) and O(¹D). Journal of Geophysical Research, 1983, 88, 4140-4144.	3.3	52
82	Joule heating in the mesosphere and thermosphere during the July 13, 1982, solar proton event. Journal of Geophysical Research, 1987, 92, 6083-6090.	3.3	50
83	Modeling studies of the impact of highâ€speed streams and coâ€rotating interaction regions on the thermosphereâ€ionosphere. Journal of Geophysical Research, 2012, 117, .	3.3	50
84	First Results From the Ionospheric Extension of WACCMâ€X During the Deep Solar Minimum Year of 2008. Journal of Geophysical Research: Space Physics, 2018, 123, 1534-1553.	0.8	50
85	Daytime climatology of ionospheric <i>N</i> _{<i>m</i>} <i>F</i> ₂ and <i>h</i> _{<i>m</i>} <i>F</i> ₂ from COSMIC data. Journal of Geophysical Research, 2012, 117, .	3.3	49
86	Seasonal variability of the OH Meinel bands. Planetary and Space Science, 1987, 35, 977-989.	0.9	48
87	New aspects of the ionospheric response to the October 2003 superstorms from multipleâ€satellite observations. Journal of Geophysical Research: Space Physics, 2014, 119, 2298-2317.	0.8	48
88	The effect of carbon dioxide cooling on trends in the F2-layer ionosphere. Journal of Atmospheric and Solar-Terrestrial Physics, 2009, 71, 1592-1601.	0.6	47
89	Simulation of polar stratospheric clouds in the specified dynamics version of the whole atmosphere community climate model. Journal of Geophysical Research D: Atmospheres, 2013, 118, 4991-5002.	1.2	47
90	Miniature X-Ray Solar Spectrometer: A Science-Oriented, University 3U CubeSat. Journal of Spacecraft and Rockets, 2016, 53, 328-339.	1.3	46

#	Article	IF	CITATIONS
91	Investigation of a Neutral "Tongue―Observed by GOLD During the Geomagnetic Storm on May 11, 2019. Journal of Geophysical Research: Space Physics, 2021, 126, e2020JA028817.	0.8	46
92	Ionospheric Day-to-Day Variability Around the Whole Heliosphere Interval in 2008. Solar Physics, 2011, 274, 457-472.	1.0	45
93	Observations and simulations of quasiperiodic ionospheric oscillations and largeâ€scale traveling ionospheric disturbances during the December 2006 geomagnetic storm. Journal of Geophysical Research, 2008, 113, .	3.3	44
94	Model simulation of thermospheric response to recurrent geomagnetic forcing. Journal of Geophysical Research, 2010, 115, .	3.3	44
95	Scientific objectives and capabilities of the Coronal Solar Magnetism Observatory. Journal of Geophysical Research: Space Physics, 2016, 121, 7470-7487.	0.8	40
96	Variations in Thermosphere Composition and Ionosphere Total Electron Content Under "Geomagnetically Quiet―Conditions at Solarâ€Minimum. Geophysical Research Letters, 2021, 48, e2021GL093300.	1.5	40
97	On the solar cycle variation of the winter anomaly. Journal of Geophysical Research: Space Physics, 2014, 119, 4938-4949.	0.8	38
98	auroral electron transport using the Monte Carlo Method. Geophysical Research Letters, 1993, 20, 185-188.	1.5	37
99	Hydrodynamic planetary thermosphere model: 2. Coupling of an electron transport/energy deposition model. Journal of Geophysical Research, 2008, 113, .	3.3	37
100	Modes of highâ€latitude auroral conductance variability derived from DMSP energetic electron precipitation observations: Empirical orthogonal function analysis. Journal of Geophysical Research: Space Physics, 2015, 120, 11,013.	0.8	37
101	New Solar Irradiance Measurements from the Miniature X-Ray Solar Spectrometer Cubesat. Astrophysical Journal, 2017, 835, 122.	1.6	37
102	TIMED Doppler Interferometer on the Thermosphere Ionosphere Mesosphere Energetics and Dynamics satellite: Data product overview. Journal of Geophysical Research, 2006, 111, .	3.3	36
103	Duration of an ionospheric data assimilation initialization of a coupled thermosphere-ionosphere model. Space Weather, 2007, 5, n/a-n/a.	1.3	36
104	New 3â€Ð simulations of climate change in the thermosphere. Journal of Geophysical Research: Space Physics, 2015, 120, 2183-2193.	0.8	36
105	Reevaluation of the O ⁺ (²P) reaction rate coefficients derived from Atmosphere Explorer C observations. Journal of Geophysical Research, 1993, 98, 15589-15597.	3.3	35
106	The role of proton precipitation in the excitation of auroral FUV emissions. Journal of Geophysical Research, 2001, 106, 21475-21494.	3.3	35
107	Response of the upper/middle atmosphere to coronal holes and powerful high-speed solar wind streams in 2003. Geophysical Monograph Series, 2006, , 319-340.	0.1	35
108	Altitude variations of the horizontal thermospheric winds during geomagnetic storms. Journal of Geophysical Research, 2008, 113, .	3.3	35

#	Article	IF	CITATIONS
109	Whole Atmosphere Climate Change: Dependence on Solar Activity. Journal of Geophysical Research: Space Physics, 2019, 124, 3799-3809.	0.8	35
110	Comparison of GOLD Nighttime Measurements With Total Electron Content: Preliminary Results. Journal of Geophysical Research: Space Physics, 2020, 125, e2019JA027767.	0.8	35
111	An investigation comparing groundâ€based techniques that quantify auroral electron flux and conductance. Journal of Geophysical Research: Space Physics, 2015, 120, 9038-9056.	0.8	34
112	Seasonal and hemispheric variations of the total auroral precipitation energy flux from TIMED/GUVI. Journal of Geophysical Research, 2010, 115, .	3.3	33
113	The summer evening anomaly and conjugate effects. Journal of Geophysical Research, 2011, 116, n/a-n/a.	3.3	33
114	Numerical models of the E-region ionosphere. Advances in Space Research, 2006, 37, 1031-1037.	1.2	31
115	A selfâ€consistent model of helium in the thermosphere. Journal of Geophysical Research: Space Physics, 2015, 120, 6884-6900.	0.8	31
116	Solar extreme ultraviolet variability of the X-class flare on 21 April 2002 and the terrestrial photoelectron response. Space Weather, 2003, 1, n/a-n/a.	1.3	30
117	Explaining solar cycle effects on composition as it relates to the winter anomaly. Journal of Geophysical Research: Space Physics, 2015, 120, 5890-5898.	0.8	30
118	Solar EUV irradiance from the San Marco Assi: A reference spectrum. Geophysical Research Letters, 1992, 19, 2175-2178.	1.5	29
119	Solar extreme ultraviolet and x-ray irradiance variations. Geophysical Monograph Series, 2004, , 127-140.	0.1	29
120	Effect of trends of middle atmosphere gases on the mesosphere and thermosphere. Journal of Geophysical Research: Space Physics, 2013, 118, 3846-3855.	0.8	29
121	Ionospheric electron densities calculated using different EUV flux models and cross sections: Comparison with radar data. Journal of Geophysical Research, 1995, 100, 14569.	3.3	28
122	Space Weather Modeling Capabilities Assessment: Neutral Density for Orbit Determination at low Earth orbit. Space Weather, 2018, 16, 1806-1816.	1.3	28
123	Observation of Postsunset OI 135.6Ânm Radiance Enhancement Over South America by the GOLD Mission. Journal of Geophysical Research: Space Physics, 2021, 126, e2020JA028108.	0.8	28
124	On Recent Large Antarctic Ozone Holes and Ozone Recovery Metrics. Geophysical Research Letters, 2021, 48, e2021GL095232.	1.5	28
125	Comparison of measured and modeled solar EUV flux and its effect on the <i>Eâ€F1</i> region ionosphere. Journal of Geophysical Research, 1992, 97, 10513-10524.	3.3	27

126 Operational performance of the TIMED Doppler Interferometer (TIDI). , 2003, , .

27

#	Article	IF	CITATIONS
127	Driving the TING model with GAIM electron densities: Ionospheric effects on the thermosphere. Journal of Geophysical Research, 2008, 113, .	3.3	27
128	Carbon dioxide trends in the mesosphere and lower thermosphere. Journal of Geophysical Research: Space Physics, 2017, 122, 4474-4488.	0.8	27
129	Solar flare effects in the Earth's magnetosphere. Nature Physics, 2021, 17, 807-812.	6.5	27
130	Local time asymmetries in the Venus thermosphere. Journal of Geophysical Research, 1993, 98, 10849-10871.	3.3	26
131	Global ionospheric total electron contents (TECs) during the last two solar minimum periods. Journal of Geophysical Research: Space Physics, 2014, 119, 2090-2100.	0.8	26
132	Globalâ€Scale Observations of the Limb and Disk Mission Implementation: 2. Observations, Data Pipeline, and Level 1 Data Products. Journal of Geophysical Research: Space Physics, 2020, 125, e2020JA027809.	0.8	26
133	Vertical variations in the N2mass mixing ratio during a thermospheric storm that have been simulated using a coupled magnetosphere-ionosphere-thermosphere model. Journal of Geophysical Research, 2006, 111, .	3.3	25
134	Meridional winds derived from COSMIC radio occultation measurements. Journal of Geophysical Research, 2008, 113, .	3.3	25
135	Effects of the equatorial ionosphere anomaly on the interhemispheric circulation in the thermosphere. Journal of Geophysical Research: Space Physics, 2016, 121, 2522-2530.	0.8	25
136	Nitrate ion spikes in ice cores not suitable as proxies for solar proton events. Journal of Geophysical Research D: Atmospheres, 2016, 121, 2994-3016.	1.2	25
137	Selfâ€Consistent Modeling of Electron Precipitation and Responses in the Ionosphere: Application to Lowâ€Altitude Energization During Substorms. Geophysical Research Letters, 2018, 45, 6371-6381.	1.5	25
138	Solar EUV and XUV energy input to thermosphere on solar rotation time scales derived from photoelectron observations. Journal of Geophysical Research, 2012, 117, .	3.3	24
139	Heating of the sunlit polar cap ionosphere by reflected photoelectrons. Journal of Geophysical Research: Space Physics, 2014, 119, 8660-8684.	0.8	24
140	New Observations of Largeâ€Scale Waves Coupling With the Ionosphere Made by the GOLD Mission: Quasiâ€16â€Day Wave Signatures in the Fâ€Region OI 135.6â€nm Nightglow During Sudden Stratospheric Warmings. Journal of Geophysical Research: Space Physics, 2020, 125, e2020JA027880.	0.8	24
141	Measurements of the solar soft X-ray irradiance from the Student Nitric Oxide Explorer. Geophysical Research Letters, 1999, 26, 1255-1258.	1.5	23
142	Observations of mesospheric neutral wind 12-hour wave in the Northern Polar Cap. Journal of Atmospheric and Solar-Terrestrial Physics, 2003, 65, 971-978.	0.6	23
143	Quantification of the spreading effect of auroral proton precipitation. Journal of Geophysical Research, 2004, 109, .	3.3	22
144	Anomalously low geomagnetic energy inputs during 2008 solar minimum. Journal of Geophysical Research, 2012, 117, .	3.3	22

#	Article	IF	CITATIONS
145	Validation of Ionospheric Specifications During Geomagnetic Storms: TEC and foF2 During the 2013 March Storm Event. Space Weather, 2018, 16, 1686-1701.	1.3	22
146	The Longâ€Term Trends of Nocturnal Mesopause Temperature and Altitude Revealed by Na Lidar Observations Between 1990 and 2018 at Midlatitude. Journal of Geophysical Research D: Atmospheres, 2019, 124, 5970-5980.	1.2	22
147	MinXSS-2 CubeSat mission overview: Improvements from the successful MinXSS-1 mission. Advances in Space Research, 2020, 66, 3-9.	1.2	22
148	Electrodynamics of magnetosphereâ€ionosphere coupling and feedback on magnetospheric field line resonances. Journal of Geophysical Research, 2007, 112, .	3.3	21
149	An improved parameterization of thermal electron heating by photoelectrons, with application to an X17 flare. Journal of Geophysical Research, 2008, 113, .	3.3	21
150	The effect of solar radio bursts on the GNSS radio occultation signals. Journal of Geophysical Research: Space Physics, 2013, 118, 5906-5918.	0.8	21
151	Thermospheric recovery during the 5 April 2010 geomagnetic storm. Journal of Geophysical Research: Space Physics, 2017, 122, 4588-4599.	0.8	21
152	Tomographic inversion of satellite photometry Part 2. Applied Optics, 1985, 24, 4134.	2.1	20
153	The visible airglow experiment—a review. Planetary and Space Science, 1988, 36, 21-35.	0.9	20
154	Auroral excitation of the N ₂ 2P(0,0) and VK(0,9) bands. Journal of Geophysical Research, 1989, 94, 17215-17222.	3.3	20
155	Temperature dependence of the reaction N2(A3â^u+)+O in the terrestrial thermosphere. Journal of Geophysical Research, 2000, 105, 10615-10629.	3.3	20
156	A "tongue―of neutral composition. Journal of Atmospheric and Solar-Terrestrial Physics, 2004, 66, 1457-1468.	0.6	19
157	Secular changes in the thermosphere and ionosphere between two quiet Sun periods. Journal of Geophysical Research: Space Physics, 2014, 119, 2255-2262.	0.8	19
158	Temporal Variability of Atomic Hydrogen From the Mesopause to the Upper Thermosphere. Journal of Geophysical Research: Space Physics, 2018, 123, 1006-1017.	0.8	19
159	Ultraviolet nightglow production near the magnetic equator by neutral particle precipitation. Journal of Geophysical Research, 1986, 91, 11365-11368.	3.3	18
160	Photoelectrons as a tool to evaluate spectral variations in solar EUV irradiance over solar cycle timescales. Journal of Geophysical Research, 2009, 114, .	3.3	18
161	Structure of the nonmigrating semidiurnal tide above Antarctica observed from the TIMED Doppler Interferometer. Journal of Geophysical Research, 2009, 114, .	3.3	18
162	Reversed ionospheric convections during the November 2004 storm: Impact on the upper atmosphere. Journal of Geophysical Research, 2009, 114, .	3.3	18

#	Article	IF	CITATIONS
163	Longitudinal variations of nighttime electron auroral precipitation in both the Northern and Southern hemispheres from the TIMED global ultraviolet imager. Journal of Geophysical Research, 2011, 116, .	3.3	18
164	CMIT study of CR2060 and 2068 comparing L1 and MAS solar wind drivers. Journal of Atmospheric and Solar-Terrestrial Physics, 2012, 83, 39-50.	0.6	18
165	The winter helium bulge revisited. Geophysical Research Letters, 2014, 41, 6603-6609.	1.5	18
166	A fast, parameterized model of upper atmospheric ionization rates, chemistry, and conductivity. Journal of Geophysical Research: Space Physics, 2015, 120, 4936-4949.	0.8	18
167	Simulation of the 21 August 2017 Solar Eclipse Using the Whole Atmosphere Community Climate Modelâ€eXtended. Geophysical Research Letters, 2018, 45, 3793-3800.	1.5	18
168	Spectral analysis of ionospheric electron density and mesospheric neutral wind diurnal nonmigrating tides observed by COSMIC and TIMED satellites. Geophysical Research Letters, 2009, 36, .	1.5	17
169	First Clobalâ€Scale Synoptic Imaging of Solar Eclipse Effects in the Thermosphere. Journal of Geophysical Research: Space Physics, 2020, 125, e2020JA027789.	0.8	17
170	Sounding rocket measurements of the solar soft X-ray irradiance. Solar Physics, 1999, 186, 243-257.	1.0	16
171	Aspects of data assimilation peculiar to space weather forecasting. Space Weather, 2006, 4, n/a-n/a.	1.3	16
172	Electromagnetic waves generated by ionospheric feedback instability. Journal of Geophysical Research, 2008, 113, .	3.3	16
173	Nitrate deposition to surface snow at Summit, Greenland, following the 9 November 2000 solar proton event. Journal of Geophysical Research D: Atmospheres, 2014, 119, 6938-6957.	1.2	16
174	Globalâ€Scale Observations and Modeling of Farâ€Ultraviolet Airglow During Twilight. Journal of Geophysical Research: Space Physics, 2020, 125, e2019JA027645.	0.8	16
175	Observations of thermospheric horizontal neutral winds at Watson Lake, Yukon Territory (Λ = 65°N). Journal of Geophysical Research, 1996, 101, 241-259.	3.3	15
176	First Synoptic Observations of Geomagnetic Storm Effects on the Global‣cale OI 135.6â€nm Dayglow in the Thermosphere by the GOLD Mission. Geophysical Research Letters, 2020, 47, e2019GL085400.	1.5	14
177	Global‣cale Observations of the Limb and Disk Mission Implementation: 1. Instrument Design and Early Flight Performance. Journal of Geophysical Research: Space Physics, 2020, 125, e2020JA027797.	0.8	14
178	Optical Aeronomy. Reviews of Geophysics, 1991, 29, 1089-1109.	9.0	13
179	Thermospheric neutral density response to solar forcing. Advances in Space Research, 2008, 42, 926-932.	1.2	13
180	A Comparative Study of Spectral Auroral Intensity Predictions From Multiple Electron Transport Models. Journal of Geophysical Research: Space Physics, 2018, 123, 993-1005.	0.8	13

#	Article	IF	CITATIONS
181	Role Of the Sun and the Middle atmosphere/thermosphere/ionosphere In Climate (ROSMIC): a retrospective and prospective view. Progress in Earth and Planetary Science, 2021, 8, .	1.1	13
182	<title>Student Nitric Oxide Explorer</title> . , 1996, , .		12
183	Brightness measurements of the nighttime O I 8446 Ã airglow emission from the Millstone Hill and Arecibo Observatories. Journal of Geophysical Research, 2000, 105, 5275-5290.	3.3	12
184	Study of the proton arc spreading effect on primary ionization rates. Journal of Geophysical Research, 2005, 110, .	3.3	12
185	Observations of the solar soft X-ray irradiance by the student nitric oxide explorer. Advances in Space Research, 2006, 37, 209-218.	1.2	12
186	Longitudinal Variation of Postsunset Plasma Depletions From the Global‧cale Observations of the Limb and Disk (GOLD) Mission. Journal of Geophysical Research: Space Physics, 2021, 126, e2020JA028510.	0.8	12
187	Vacuum-ultraviolet instrumentation for solar irradiance and thermospheric airglow. Optical Engineering, 1994, 33, 438.	0.5	11
188	Calibration of the San Marco airglowâ€solar spectrometer instrument in the extreme ultraviolet. Optical Engineering, 1996, 35, 554.	0.5	11
189	Neutral Exospheric Temperatures From the GOLD Mission. Journal of Geophysical Research: Space Physics, 2020, 125, e2020JA027814.	0.8	11
190	Responses of the Thermosphere and Ionosphere System to Concurrent Solar Flares and Geomagnetic Storms. Journal of Geophysical Research: Space Physics, 2020, 125, e2019JA027431.	0.8	11
191	The OI 989â€Ã tropical nightglow. Geophysical Research Letters, 1984, 11, 569-571.	1.5	10
192	Recent observations of the OI 8446 Ã emission over Millstone Hill. Geophysical Research Letters, 1994, 21, 829-832.	1.5	10
193	Multi-year high latitude mesospheric neutral wind observations using a Fabry–Perot interferometer. Advances in Space Research, 2005, 35, 1895-1899.	1.2	10
194	The TIGER (thermospheric–ionospheric geospheric research) program: Introduction. Advances in Space Research, 2006, 37, 194-198.	1.2	10
195	An analysis of neutral wind generated currents during geomagnetic storms. Journal of Atmospheric and Solar-Terrestrial Physics, 2007, 69, 159-165.	0.6	10
196	Where does the Thermospheric Ionospheric GEospheric Research (TIGER) Program go?. Advances in Space Research, 2015, 56, 1547-1577.	1.2	10
197	Solar cycle variations of thermospheric composition at the solstices. Journal of Geophysical Research: Space Physics, 2016, 121, 3740-3749.	0.8	10
198	Quantifying the Storm Time Thermospheric Neutral Density Variations Using Model and Observations. Space Weather, 2019, 17, 269-284.	1.3	10

#	Article	IF	CITATIONS
199	Thermosphere-Ionsphere-Mesosphere Energetics and Dynamics (TIMED) Solar EUV Experiment. , 1994, 2266, 467.		9
200	A new inversion for Stratospheric Aerosol and Gas Experiment II data. Journal of Geophysical Research, 1998, 103, 8465-8475.	3.3	9
201	Observation of the mesospheric and lower thermospheric 10-hour wave in the northern polar region. Journal of Geophysical Research, 2002, 107, SIA 4-1.	3.3	9
202	Impact of solar EUV, XUV, and X-Ray variations on Earths's atmosphere. Geophysical Monograph Series, 2004, , 341-354.	0.1	9
203	High-resolution, coupled thermosphere–ionosphere models for space weather applications. Advances in Space Research, 2005, 36, 2486-2491.	1.2	9
204	A high-latitude 8-hour wave in the mesosphere and lower thermosphere. Journal of Geophysical Research, 2005, 110, .	3.3	9
205	Longitudinal variations of thermospheric composition at the solstices. Journal of Geophysical Research: Space Physics, 2016, 121, 6818-6829.	0.8	9
206	Upper Atmosphere Radiance Data Assimilation: A Feasibility Study for GOLD Far Ultraviolet Observations. Journal of Geophysical Research: Space Physics, 2019, 124, 8154-8164.	0.8	9
207	Climate Changes in the Upper Atmosphere: Contributions by the Changing Greenhouse Gas Concentrations and Earth's Magnetic Field From the 1960s to 2010s. Journal of Geophysical Research: Space Physics, 2021, 126, e2020JA029067.	0.8	9
208	Influence of Space Weather on Aircraft Ionizing Radiation Exposure. , 2008, , .		8
209	Unusual declining phase of solar cycle 23: Weak semiâ€∎nnual variations of auroral hemispheric power and geomagnetic activity. Geophysical Research Letters, 2009, 36, .	1.5	8
210	Global-Scale Observations of the Limb and Disk (Gold): New Observing Capabilities for the Ionosphere-Thermosphere. Geophysical Monograph Series, 0, , 319-326.	0.1	8
211	Simulations of the equatorial thermosphere anomaly: Geomagnetic activity modulation. Journal of Geophysical Research: Space Physics, 2014, 119, 6821-6832.	0.8	8
212	Thermospheric hydrogen response to increases in greenhouse gases. Journal of Geophysical Research: Space Physics, 2016, 121, 3545-3554.	0.8	8
213	Observation of Thermospheric Gravity Waves in the Southern Hemisphere With GOLD. Journal of Geophysical Research: Space Physics, 2020, 125, e2019JA027405.	0.8	8
214	Effects of EMIC Waveâ€Driven Proton Precipitation on the Ionosphere. Journal of Geophysical Research: Space Physics, 2022, 127, .	0.8	8
215	An event study to provide validation of TING and CMIT geomagnetic middleâ€latitude electron densities at the F ₂ peak. Journal of Geophysical Research, 2008, 113, .	3.3	7
216	Wavelength dependence of solar irradiance enhancement during X-class flares and its influence on the upper atmosphere. Journal of Atmospheric and Solar-Terrestrial Physics, 2014, 115-116, 87-94.	0.6	7

#	Article	IF	CITATIONS
217	Ionospheric Electron Content During Solar Cycle 23. Journal of Geophysical Research: Space Physics, 2018, 123, 5223-5231.	0.8	7
218	Spectroscopy, gas kinetics, and opacity of thermospheric nitric oxide and implications for analysis of SABER infrared emission measurements at 5.3 Âμm. Journal of Quantitative Spectroscopy and Radiative Transfer, 2021, 268, 107609.	1.1	7
219	Science instrumentation for the Student Nitric Oxide Explorer. , 1996, 2830, 264.		6
220	First Comparison of Traveling Atmospheric Disturbances Observed in the Middle Thermosphere by Globalâ€Scale Observations of the Limb and Disk to Traveling Ionospheric Disturbances Seen in Groundâ€Based Total Electron Content Observations. Journal of Geophysical Research: Space Physics, 2021, 126, e2021JA029248.	0.8	6
221	Electron-impact excitation/emission and photoabsorption cross sections important in the terrestrial airglow and auroral analysis of rocket and satellite observations. Physics and Chemistry of the Earth, Part C: Solar, Terrestrial and Planetary Science, 2000, 25, 573-581.	0.2	5
222	Incoherent scatter radar measurements and modeling of high-latitude solar photoionization. Journal of Geophysical Research, 2005, 110, .	3.3	4
223	Space Weather Nowcasting of Atmospheric Ionizing Radiation for Aviation Safety. , 2007, , .		4
224	Building and Using Coupled Models for the Space Weather System: Lessons Learned. Space Weather, 2009, 7, n/a-n/a.	1.3	4
225	On deriving incident auroral particle fluxes in the daytime using combined ground-based optical and radar measurements. Journal of Geophysical Research, 2011, 116, n/a-n/a.	3.3	4
226	Imaging spectroscopy for two-dimensional characterization of auroral emissions. Applied Optics, 1998, 37, 5760.	2.1	3
227	Enhancement of OI 630.0nm emission at mid-latitudes during an intense magnetic storm. Journal of Atmospheric and Solar-Terrestrial Physics, 2007, 69, 697-706.	0.6	3
228	Variations of Lower Thermospheric FUV Emissions Based on GOLD Observations and GLOW Modeling. Journal of Geophysical Research: Space Physics, 2020, 125, e2020JA027810.	0.8	3
229	Mesospheric ionization and depletion. Planetary and Space Science, 1987, 35, 1087-1091.	0.9	2
230	Solar extreme ultraviolet irradiance measurements from sounding rockets during solar cycle 22. Physics and Chemistry of the Earth, Part C: Solar, Terrestrial and Planetary Science, 2000, 25, 397-399.	0.2	2
231	Modeling of the thermosphere-ionosphere system. Physics and Chemistry of the Earth, Part C: Solar, Terrestrial and Planetary Science, 2000, 25, 499-503.	0.2	2
232	RENU2 UV PMT Observations of the Cusp. Geophysical Research Letters, 2020, 47, e2019GL082314.	1.5	2
233	Comment on "Atmospheric ionization by highâ€fluence, hard spectrum solar proton events and their probable appearance in the ice core archive―by A. L. Melott et al Journal of Geophysical Research D: Atmospheres, 2016, 121, 12,484.	1.2	1
234	Trends in the Neutral and Ionized Upper Atmosphere. Space Sciences Series of ISSI, 2011, , 113-145.	0.0	1

#	Article	IF	CITATIONS
235	Thermospheric Density: An Overview of Temporal and Spatial Variations. Space Sciences Series of ISSI, 2011, , 147-173.	0.0	1